Interactions of *N*-Stearoyl Sphingomyelin with Cholesterol and Dipalmitoylphosphatidylcholine in Bilayer Membranes

P. R. Maulik and G. G. Shipley
Departments of Biophysics and Biochemistry, Boston University School of Medicine, Center for Advanced Biomedical Research, Boston, Massachusetts 02118 USA

ABSTRACT Differential scanning calorimetry and x-ray diffraction have been utilized to investigate the interaction of N-stearoylsphingomyelin (C18:0-SM) with cholesterol and dipalmitoylphosphatidylcholine (DPPC). Fully hydrated C18:0-SM forms bilayers that undergo a chain-melting (gel → liquid-crystalline) transition at 45°C, ΔH = 6.7 kcal/mol. Addition of cholesterol results in a progressive decrease in the enthalpy of the transition at 45°C and the appearance of a broad transition centered at 46.3°C; this latter transition progressively broadens and is not detectable at cholesterol contents of >40 mol%. X-ray diffraction and electron density profiles indicate that bilayers of C18:0-SM/cholesterol (50 mol%) are essentially identical at 22°C and 58°C in terms of bilayer periodicity (d = 63–64 Å), bilayer thickness ($d_{p\text{-}p}$ = 46–47 Å), and lateral molecular packing (wide-angle reflection, ~1/4.8 $Å^{-1}$). These data show that cholesterol inserts into C18:0-SM bilayers, progressively removing the chain-melting transition and altering the bilayer structural characteristics. In contrast, DPPC has relatively minor effects on the structure and thermotropic properties of C18:0-SM. DPPC and C18:0-SM exhibit complete miscibility in both the gel and liquid-crystalline bilayer phases, but the pre-transition exhibited by DPPC is eliminated at >30 mol% C18:0-SM. The bilayer periodicity in both the gel and liquid-crystalline phases decreases significantly at high DPPC contents, probably reflecting differences in hydration and/or chain tilt (gel phase) of C18:0-SM and DPPC.

INTRODUCTION

The lipid bilayer matrix of many plasma membranes consists of glycerophospholipids (e.g., phosphatidylcholine, phosphatidylethanolamine, phosphatidylserine), sphingolipids (e.g., sphingomyelin, cerebroside, gangliosides), and cholesterol. The specific role of cholesterol is to regulate the order and fluidity of the lipid bilayer compartment. The lipid bilayer serves as a matrix in which membrane proteins are incorporated with a specific molecular orientation to fulfill their receptor, transport, and enzymatic functions. Among the more polar glycerophospholipids and sphingolipids, the two choline-containing phospholipids, phosphatidylcholine (PC) and sphingomyelin (SM), are found in relatively large amounts in many cell membranes. In addition, the lipid bilayer itself appears to maintain an asymmetric disposition with respect to its polar lipid constituents. For example, there is a preferential location of PC and SM on the external monolayer of the red cell membrane. Furthermore, the polar lipids PC and SM are located at the outer surface of plasma lipoprotein particles where, together with unesterified cholesterol, they form monolayers into which functional apoproteins are incorporated. This lipid-protein monolayer surrounds a spherical, nonpolar core of cholesterol ester and/or triglyceride and thus maintains the overall stability and structure of lipoprotein particles such as high-density lipoprotein and low-density lipoprotein.

Apart from its structural role, SM appears to be involved in specific cellular processes. For example, SM or other sphingolipids are thought to be required for the fusion of the enveloped Semliki forest virus to target membranes (Nieva et al., 1994). Furthermore, it has been shown that SM is involved in a receptor-mediated signaling pathway (for reviews, see Hannun, 1994; Hannun and Obeid, 1995). After ligand binding to membrane receptors, activation of a membrane sphingomyelinase converts SM to ceramide by removal of the phosphorylcholine group. The released ceramide acts as a second messenger through stimulation of both protein kinase and protein phosphatase pathways; these processes, in turn, are thought to contribute to the regulation of both cell growth and apoptosis.

A vast literature exists describing 1) the thermotropic properties and structure of hydrated PC and 2) its interaction with other lipids, notably cholesterol. In contrast, relatively few physical studies of SM have been made (for reviews, see Barenholz and Thompson, 1980; Barenholz and Gatt, 1982). Our initial differential scanning calorimetry (DSC) and x-ray diffraction study of bovine brain SM (Shipley et al., 1974) showed that its ordered gel → liquid-crystal transition occurred at a surprisingly high temperature for a naturally occurring lipid (30–40°C); similar behavior was later reported by Barenholz et al. (1976). Early studies of bovine brain SM-cholesterol interactions detected by DSC (Oldfield and Chapman, 1971; L. S. Avecilla and G. G. Shipley, unpublished observations), nuclear magnetic resonance (NMR) (Oldfield and Chapman, 1972), electron spin resonance (Long et al., 1971), and x-ray diffraction (Khare and Worthington, 1977; L. S. Avecilla and G. G. Shipley,

Received for publication 30 October 1995 and in final form 29 January 1996.

Address reprint requests to Dr. G. Graham Shipley, Departments of Biophysics and Biochemistry, Boston University School of Medicine, Center for Advanced Biomedical Research, 80 East Concord Street, Boston, MA 02118. Tel.: 617-638-4009; Fax: 617-638-4041; E-mail: shipley@med-biophi.bu.edu.

0006-3495/96/05/2256/10 $2.00

unpublished observations) showed that the addition of cholesterol to SM removes the chain-melting transition, fluidizes/disorders the bilayer below the original phase transition, and makes it less fluid above the transition temperature. Furthermore, in view of the coexistence (and colocalization) of SM and PC in cell membranes and plasma lipoproteins, we studied the binary lipid system of bovine brain SM-egg yolk PC by x-ray diffraction, DSC, and polarizing light microscopy (Untracht and Shipley, 1977). This study showed that the high chain-melting temperature of SM leads to lateral phase separation as hydrated mixtures of SM and PC are cooled to temperatures below ~40°C.

The interpretation of the results obtained from the studies of naturally occurring bovine brain SM and its interaction with PC and cholesterol are complicated by the chemical heterogeneity of the amide-linked fatty acid (see Calhoun and Shipley, 1979a) and, to a lesser extent, the sphingosine base composition. This has led to 1) the development of synthetic protocols in which specific amide-linked fatty acids are incorporated into SM by deacylation-reacylation methods (Calhoun and Shipley, 1979b; Cohen et al., 1984; Ahmad et al., 1985; Sripada et al., 1987), and 2) the de novo synthesis of chemically and stereochemically pure SM (Shapiro, 1969; Bruzik, 1988a; Dong and Butcher, 1993).

Studies of the physical properties of synthetic SM have now been reported. For example, DSC was used to investigate the thermotropic behavior of synthetic C16:0-, C18:0-, and C24:0-SM with the sphingosine in the DL-erythro configuration (Barenholz et al., 1976) and the interactions of these synthetic SM with cholesterol (Estep et al., 1979, 1981). Hydrated C16:0-SM showed a simple, reversible gel → liquid crystal transition at ~41°C, whereas C18:0-SM showed two low-temperature bilayer forms: a stable bilayer phase that melts at 57°C and a metastable bilayer phase melting at 44°C (Estep et al., 1980). The longer chain C24:0-SM exhibited more complex thermotropic behavior, with a transition at 42.6°C followed by the main transition at 48.6°C. Interaction of cholesterol with C18:0-SM resulted in two distinct transitions at ~56–57°C and 43–45°C, suggesting that a cholesterol-rich phase coexists with a cholesterol-poor phase when the cholesterol content is low (<20 mol%). Similar cholesterol effects were observed with C16:0- and C24:0-SM. More recently, Bruzik and colleagues have studied the properties of stereochemically pure isomers of SM (Bruzik, 1988a) using DSC (Bruzik and Tsai, 1987) and NMR (Bruzik, 1988b; Bruzik et al., 1990) methods. For example, D-erythro-C18:0-SM exhibits a chain-melting transition at ~45°C and can adopt several low-temperature gel phases depending on the thermal history (Bruzik and Tsai, 1987).

Our own studies focused initially on C16:0-SM synthesized by deacylation and reacylation of bovine brain SM (Calhoun and Shipley, 1979b). DSC showed that hydrated C16:0-SM exhibits a reversible bilayer gel → bilayer liquid-crystal transition at 40.5°C. In addition, C16:0-SM was shown to be completely miscible with dimyristoyl PC in both the gel and liquid-crystal phases. In contrast to immiscible SM-PC systems, where cholesterol appears to have higher affinity for SM (Demel et al., 1977), no preferential affinity for either C16:0-SM or dimyristoyl PC was found in the miscible system (Calhoun and Shipley, 1979b).

We then extended our partial synthesis of SM to include C14:0-, C16:0-, C18:0-, C20:0-, C22:0-, C24:0-, and C24:1-SM, and initial DSC studies showed, in contrast to the diacyl PC series, that the thermotropic behavior of some members of these SM series were complex (Sripada et al., 1987). Whereas C16:0-, C18:0-, and C20:0-SM show a single, reversible chain-melting transition between bilayer gel and liquid-crystal phases, the short-chain (C14:0) and long-chain (C22:0 and C24:0) SM exhibit more complex thermotropic behavior with multiple transitions, presumably because of a mismatch in the length of the *N*-acyl and sphingosine chains affecting molecular packing in the gel phase (Sripada et al., 1987). Although our x-ray scattering studies of single-bilayer vesicles made from this series of SM show a linear dependence of bilayer thickness on SM N-acyl chain length, there is evidence that perturbations to the bilayer packing due to chain mismatch also occur in the liquid-crystalline state (Maulik et al., 1986).

More recently we have described the structure and thermotropic properties of two members of the above series, C18:0-SM (Maulik et al., 1991) and C24:0-SM (Maulik and Shipley, 1995). For example, fully hydrated C18:0-SM exhibits a reversible gel → liquid-crystal transition at 45°C (ΔH = 6.7 kcal/mol); in the present paper we describe the interaction of cholesterol and dipalmitoylphosphatidylcholine (DPPC) with the now characterized C18:0-SM bilayers.

MATERIALS AND METHODS

Materials

C18:0-SM was prepared by partial synthesis from bovine brain SM (Calbiochem-Behring Diagnostic, San Diego, CA) as described by Sripada et al. (1987). Briefly, acid hydrolysis of bovine brain SM containing heterogeneous *N*-acyl chains produced sphingosylphosphorylcholine (SPC). C18:0-SM was obtained after reacylation of SPC using stearoyl imidazolide to *O*-*N*-distearoyl SPC, followed by hydrolysis of the *O*-ester bond. The resulting C18:0-SM was shown to be >99% pure by a combination of thin-layer chromatography and high-performance liquid chromatography. However, as noted previously (Sripada et al., 1987; Maulik et al., 1991; Maulik and Shipley, 1995), epimerization at C-3 of sphingosine does occur during the acid hydrolysis step, leading to the formation of some of the L-threo stereoisomer of SPC. Because we have not been able to separate the stereoisomers of either SPC or the reacylated SM, the desired product, D-erythro-SM, does contain ~25% of the L-threo isomer (for a detailed discussion of this issue for C16:0-SM, see Sripada et al., 1987). For the starting material, bovine brain SM, the predominant sphingosine base is C18:1t (90.2%) plus minor amounts of C20:1t (7.3%) and C18:0 (2.6%). In our detailed study of C16:0-SM (Sripada et al., 1987), C18:1t is retained as the major sphingosine base (85.7%), with changes occurring in the levels of the minor sphingosine components. A similar sphingosine profile is to be expected for C18:0-SM, in which C18:1t is the predominant (~90%) molecular species.

Cholesterol and DPPC were purchased from Nu Chek Prep (Austin, MN) and Avanti Polar Lipids (Birmingham, AL), respectively. The lipids were shown to be >99% pure by thin-layer chromatography using the solvent systems hexane/ethyl ether/acetic acid (70:30:1 v/v/v for choles-

terol) and chloroform/methanol/water/acetic acid (65:25:4:1 v/v/v/v for DPPC); thus they were used without further purification.

Differential scanning calorimetry

C18:0-SM with various molar ratios of cholesterol or DPPC were directly weighed in DSC stainless steel pans and then dissolved in chloroform/methanol (2:1 v/v). The solvent was evaporated under a slow nitrogen stream, and the sample was placed in a vacuum overnight. The DSC pans were reweighed to make sure that the total amount of lipid remained the same. Using a Hamilton syringe, an excess (50–75 wt%) of doubly distilled, deionized water was added to each sample to prepare the binary mixtures of C18:0-SM/cholesterol and C18:0-SM/DPPC. The DSC pans were hermetically sealed and placed in a Perkin-Elmer (Norwalk, CT) DSC-2 scanning calorimeter. Repeated heating and cooling scans of the samples at a rate of 5°C/min (2.5°C where appropriate) were performed over the temperature range 0 to 80°C. The peak maximum in the plot of excess heat capacity versus temperature was recorded as the transition temperature T_m; the transition enthalpies were calculated by measuring the area under the transition endotherm peak and comparing with that of a gallium standard.

X-ray diffraction

Samples of C18:0-SM containing various molar ratios of cholesterol or DPPC were weighed in constricted glass tubes and then dissolved in chloroform/methanol (2:1 v/v). The solvent was evaporated under nitrogen, and the sample was placed overnight in a vacuum. The tubes were reweighed to check for any loss of lipid. Doubly distilled, deionized water was added using a Hamilton syringe to make binary lipid mixtures (C18:0-SM/cholesterol; C18:0-SM/DPPC) in excess water (50–60 wt%), and the tubes were flame-sealed immediately. The equilibration of the multilamellar lipid/water system was achieved by repeated centrifugation of the sample through the central constriction for 5–6 h at temperatures 10°C above the phase transition temperature. The sample tubes were then opened and the samples were promptly transferred into quartz capillaries (internal diameter, 1.0 mm), and the capillary tubes were flame-sealed immediately.

X-ray diffraction patterns were recorded on photographic film using focusing cameras with either toroidal mirror (Elliot, 1965) or double mirror (Franks, 1958) optics and using nickel-filtered CuK_α radiation (λ = 1.5418 Å) generated by an Elliot GX6 rotating anode generator (Elliot Automation, Borehamwood, England). The x-ray diffraction patterns were recorded at 22°C and 58°C, as well as at other temperatures where necessary. Bilayer periodicities, d, were calculated from the lamellar reflections. The diffraction intensities were obtained using a Joyce-Loebl (Gateshead, England) model IIICS scanning microdensitometer. The observed intensities of the lamellar low-angle reflections were corrected for the Lorentz factors, scaled, normalized, and converted to structure amplitudes $F(s)$ as described by Worthington and Blaurock (1969).

X-ray diffraction data were also recorded with a position-sensitive linear detector (Tennelec, Oak Ridge, TN) and associated electronics (Tracor Northern, Middleton, WI). Nickel-filtered CuK_α x-radiation generated by a microfocus, x-ray generator (Jarrel-Ash, Waltham, MA) was line focused (100 μm × 10 mm) by a single mirror and collimated with the slit optical system of a Luzzati-Baro camera (E^{TS} Beaudoin, Paris).

RESULTS

Hydrated C18:0-SM

Fig. 1 shows DSC heating/cooling scans (5°C/min) of fully hydrated (56 wt% water) C18:0-SM multibilayers. The initial heating scan over the temperature range 0–77°C after low-temperature incubation (Fig. 1 *a*) shows a single sharp endothermic transition at 45°C (ΔH = 6.7 kcal/mol). Subsequent cooling and reheating scans (Fig. 1, *b* and *c*) confirm the reversibility of this transition. X-ray diffraction patterns of hydrated (60 wt% water) C18:0-SM were recorded at temperatures below (22°C) and above (58°C) this phase transition (Fig. 2). The low-angle region at both temperatures shows a series of lamellar reflections (h =

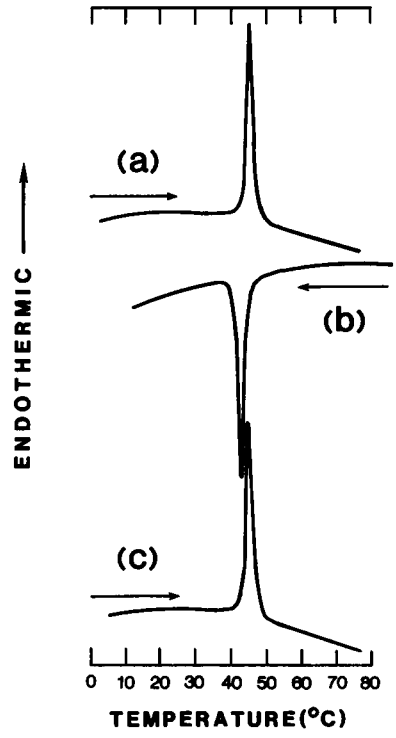

FIGURE 1 DSC heating and cooling scans of hydrated (56 wt % water) C18:0-SM. (*a*) Initial heating scan after 16-h incubation at −4°C; (*b*) immediate cooling scan; (*c*) immediate re-heating scan. Heating/cooling scan rates, 5°C/min.

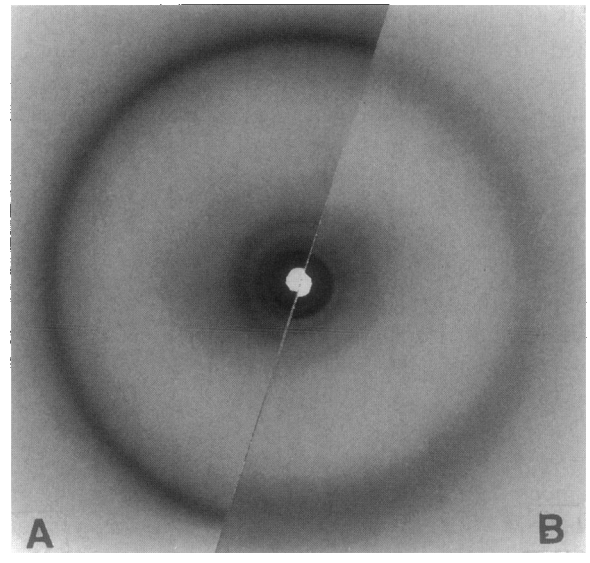

FIGURE 2 X-ray diffraction patterns of hydrated (60 wt% water) C18:0-SM at 22°C (*a*) and 58°C (*b*). Recorded using toroidal x-ray optics.

1–4) characteristic of bilayer phases, whereas the wide-angle region exhibits a sharp 1/4.2 $Å^{-1}$ at 22°C (Fig. 2 *a*) and a diffuse 1/4.5 $Å^{-1}$ reflection at 58°C (Fig. 2 *b*), corresponding to ordered chain-packing and melted-chain states, respectively. Clearly, the reversible transition of hydrated C18:0-SM corresponds to a bilayer gel → liquid-crystal transition (for more details of the hydration-dependent behavior of C18:0-SM, see Maulik et al., 1991).

Interaction of C18:0-SM with cholesterol

DSC heating scans of fully hydrated (75 wt% water) C18:0-SM containing increasing mol% cholesterol are shown in Fig. 3. At 5 mol% cholesterol, the C18:0-SM transition broadens, decreases slightly in temperature to 44°C, and decreases in enthalpy (H = 5.3 kcal/mol). As the cholesterol content increases (10–20 mol%), the transition broadens further and a higher temperature transition appears as a shoulder on the original transition. Further addition of cholesterol (26–30 mol%) leads to progressive reduction of the enthalpy of the original sharp 45°C transition and further broadening of the high-temperature transition. Finally, at cholesterol contents >40 mol%, no cooperative transition is detected. A plot of the total transition enthalpy as a function of mol% cholesterol is shown in Fig. 4. Initially, the transition enthalpy of C18:0-SM appears to decrease linearly with cholesterol content, but at higher cholesterol content a more complex dependence is suggested.

As shown in Fig. 3, at 15 mol% cholesterol the sharp peak of C18:0-SM shifts from 45°C to 43.5°C, with the broad shoulder centered at 46.3°C. To confirm the presence of the two transitions, this sample was reexamined at a slower heating/cooling scan rate. DSC heating/cooling scans (2.5°C/min) of hydrated (75 wt% water) C18:0-SM containing 15 mol% cholesterol were recorded. Again, two transitions are observed on heating (43.5°C and 46.3°C) and cooling (data not shown). The two transitions are reversible, suggesting that two gel phases coexist at low temperatures. However, the x-ray diffraction pattern recorded at 22°C indicates the presence of only a single bilayer gel phase (bilayer periodicity, d = 73.7 Å; wide-angle reflection at 1/4.2 $Å^{-1}$) below the two transitions (data not shown).

X-ray diffraction data were recorded at 22°C and 58°C from hydrated (60 wt% water) C18:0-SM containing different mol% cholesterol (0–60 mol% cholesterol). The bilayer periodicity d at 22°C and 58°C is plotted as a function of mol% cholesterol in Fig. 5. At 22°C, the bilayer periodicity of C18:0-SM increases from 74.8 Å to 76.2 Å in the presence of 10 mol% cholesterol; on further increase in the

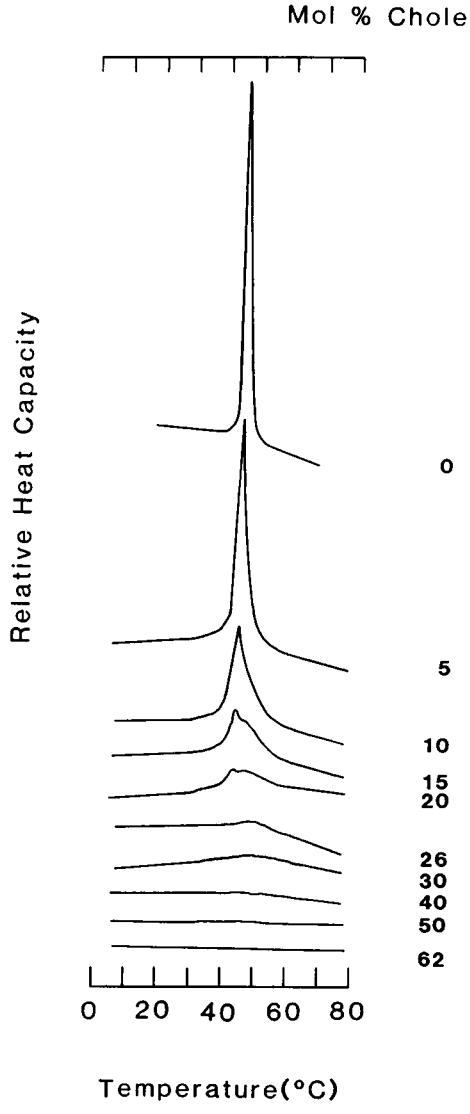

FIGURE 3 DSC heating scans of fully hydrated (75 wt% water) C18:0-SM containing 0, 5, 10, 15, 20, 26, 30, 40, 50 and 62 mol% cholesterol. Heating scan rate, 5°C/min.

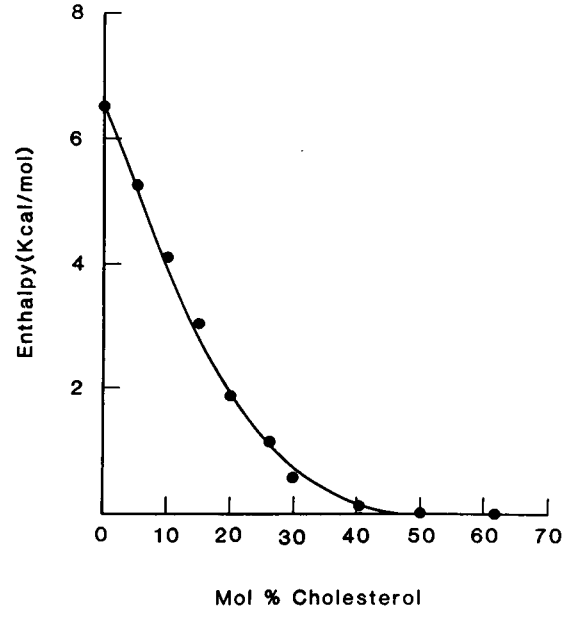

FIGURE 4 Transition enthalpy of the chain-melting transition of C18:0-SM as a function of mol% cholesterol.

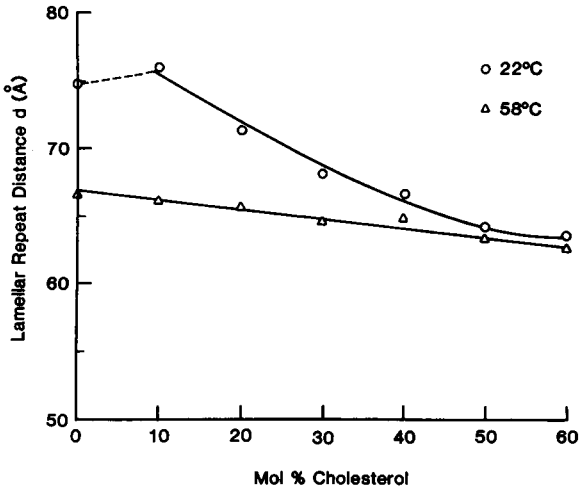

FIGURE 5 Bilayer periodicity, d (Å), of hydrated (60 wt% water) C18:0-SM/cholesterol mixtures as a function of mol% cholesterol at 22°C (○) and 58°C (△).

cholesterol content, the bilayer periodicity decreases until a limiting value of 64.2 Å is reached at ~50 mol% cholesterol (Fig. 5). A sharp 1/4.2 $Å^{-1}$ wide-angle reflection is observed for C18:0-SM at 22°C; this reflection progressively shifts and broadens, reaching a limiting value of 1/4.8 $Å^{-1}$ at ~50 mol% cholesterol (data not shown). At 58°C, the bilayer periodicity decreases linearly from 66.6 Å to 62.7 Å with increasing cholesterol content (Fig. 5), while the diffuse wide-angle reflection progressively shifts from 1/4.6 $Å^{-1}$ to 1/4.8 $Å^{-1}$ (data not shown). X-ray diffraction patterns of C18:0-SM containing 50 mol% cholesterol observed at 22°C and 58°C are shown in Fig. 6, *a* and *b*, respectively. It is clear that the two diffraction patterns are essentially identical in both bilayer periodicity and in the position and width of the wide-angle reflection.

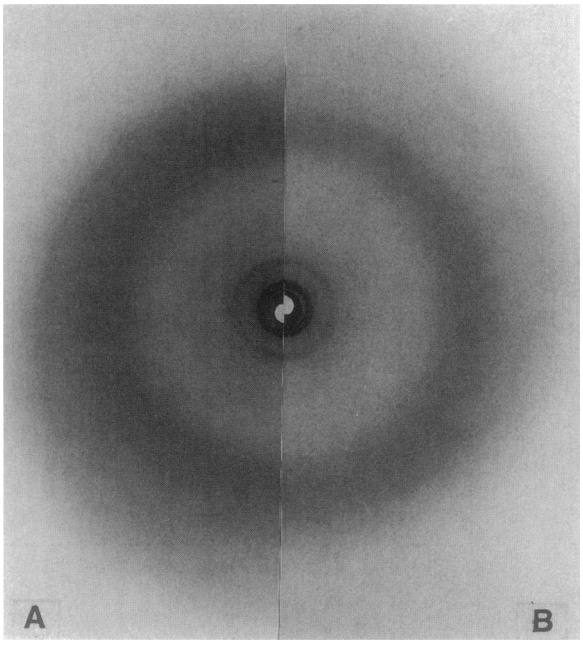

FIGURE 6 X-ray diffraction patterns of hydrated C18:0-SM/cholesterol (50 mol%) at 22°C (*a*) and 58°C (*b*). Recorded using toroidal x-ray optics.

To define further the C18:0-SM bilayer structure in the presence of cholesterol, electron density profiles, $\rho(x)$, across the SM bilayer containing 50 mol% cholesterol at 22°C and 58°C have been calculated. These profiles are compared with those of fully hydrated (40 wt% water) C18:0-SM bilayers in Fig. 7. For C18:0-SM, the phases of the corrected structure amplitudes (h = 1–4) at 22°C and 58°C were as determined previously (Maulik et al., 1991); for C18:0-SM/cholesterol (50 mol%) the phase sequence (−, −, +, +) determined for for C18:0-SM at 58°C was assumed. The centrosymmetric profiles for C18:0-SM and C18:0-SM/cholesterol show a pronounced central trough corresponding to the bilayer center (X = 0 Å) and two symmetry-related peaks corresponding to the location of the electron-rich phosphate groups. The separation of the two peaks, $d_{p\text{-}p}$, provides a measure of the bilayer thickness, i.e., lipid thickness. At 22°C, $d_{p\text{-}p}$ decreases from 52 Å (C18:0-SM) to 46.6 Å (50 mol% cholesterol), indicating a thinning of the bilayer as cholesterol is incorporated. A decrease in interbilayer separation (defined as water thickness, d_w) from 21.4 Å to 17.8 Å also occurs. In contrast, at 58°C, $d_{p\text{-}p}$ increases from 43 Å to 46 Å when 50 mol% cholesterol is present. The bilayer profiles of C18:0-SM containing 50 mol% cholesterol at 22°C and 58°C are essentially identical in shape (note the pronounced shoulder at ±10 Å due to the sterol ring system) and derived bilayer parameters $d_{p\text{-}p}$ (46–47 Å) and d_w (~18 Å).

Interaction of C18:0-SM with DPPC

DSC heating of fully hydrated (75 wt% water) C18:0-SM bilayers containing different mol% DPPC (range 0–100 mol% DPPC) are shown in Fig. 8. Fully hydrated DPPC exhibits two transitions at 35°C and 42°C corresponding to the pre-transition and chain-melting transition, whereas C18:0-SM exhibits a single, reversible chain-melting transition at 45°C (see Fig. 1 and Maulik et al., 1991). The addition of 10 mol% DPPC decreases the chain-melting temperature of C18:0-SM to 43°C; increasing the DPPC content results in only a minor decrease in the transition temperature to 42°C (Figs. 8 and 9). Some broadening of the transition is observed at intermediate DPPC contents. Over the range 0–100 mol% DPPC, the transition enthalpy increases continuously from 6.7 to 8.0 kcal/mol lipid (data not shown). In addition, at >60 mol% DPPC the pre-transition characteristic of DPPC is present, increasing in transition temperature from 28°C to 35°C (Figs. 8 and 9) and transition enthalpy from 0.1 to 0.9 kcal/mol lipid (data not shown), over the range 60–100 mol% DPPC.

X-ray diffraction data were recorded for fully hydrated (50 wt% water) binary lipid mixtures of C18:0-SM/DPPC containing 0, 25, 50, 75, 85, and 100 mol% DPPC at temperatures below (22°C) and above (58°C) the chain-

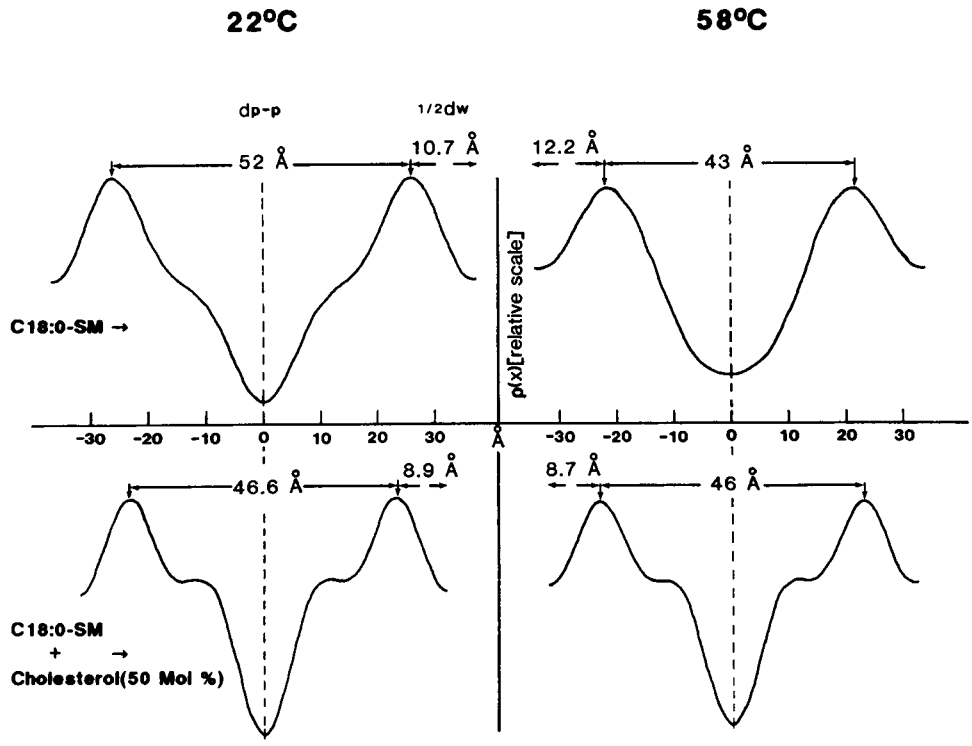

FIGURE 7 Electron density profiles of C18:0-SM (*top*) and C18:0-SM/cholesterol (50 mol%) (*bottom*) at 22°C (*left*) and 58°C (*right*).

melting transition and, where necessary, at temperatures between the pre- and main transitions. For example, x-ray diffraction of fully hydrated C18:0-SM containing 25 mol% DPPC at 22°C shows lamellar reflections (h = 1–4), bilayer periodicity (d = 76.9 Å), together with a sharp wide-angle reflection at $1/4.2^{-1}$ (data not shown). At 58°C, lamellar reflections (h = 1–5; d = 66 Å) are present, together with a diffuse wide-angle reflection at $1/4.5^{-1}$ (data not shown). X-ray diffraction patterns of all C18:0-SM/DPPC mixtures exhibit similar behavior, confirming the presence of bilayer gel and bilayer liquid-crystalline phases at 22°C and 58°C, respectively. The bilayer periodicity of C18:0-SM/DPPC mixtures is plotted as a function of mol% DPPC in Fig. 10. At 22°C, there is no significant change in bilayer periodicity (75–77 Å) up to 50 mol% DPPC; at higher DPPC contents the bilayer periodicity decreases, reaching a value of 64 Å for DPPC. At 58°C, the bilayer periodicity is essentially constant, 65 Å, up to 50 mol% DPPC. Further addition of DPPC leads to a small increase in d to 69.4 Å at 75 mol% DPPC, followed by a progressive decrease to 59 Å at 100 mol% DPPC. At temperatures between the pre-transition and chain-melting transition, bilayer reflections characteristic of the rippled phase of DPPC are observed for binary mixtures containing 70–100 mol% DPPC; the bilayer periodicity decreases from 80 to 66 Å (see Fig. 10).

DISCUSSION

Studies of the properties and interactions of sphingomyelin have attracted interest given 1) their structural contribution to the surface lipid matrices of membranes and plasma lipoproteins, and 2) their involvement in cell signaling processes. For the former, the colocalization of SM with its glycerolipid counterpart (PC) and cholesterol in the outer monolayer of many cell membrane bilayers and the surface monolayer of high-density lipoprotein, low-density lipoprotein, etc., has provided the stimulus for studies of the mutual interactions of these lipid classes.

We have reported previously on the hydration dependence of the structure and thermotropic properties of C18:0-SM (Maulik et al., 1991). Using DSC and x-ray diffraction data we have shown that hydrated C18:0-SM undergoes reversible chain melting at 45°C corresponding to a bilayer gel → bilayer liquid-crystal structural transition (Figs. 1 and 2; see Maulik et al., 1991). This thermotropic and structural behavior of the sphingosine-based C18:0-SM is similar to that of the much-studied glycerol-based PCs of different chain length. SM and PC containing the identical phosphorylcholine polar group exhibit similar limited hydration (or swelling) properties, and both favor the formation of bilayer (rather than nonbilayer hexagonal, cubic, or micellar) structures in both their gel and liquid-crystalline phases.

Similarly, there is an extensive literature describing both the molecular interactions of cholesterol with PC and the interactions between PCs of different chain length. In contrast, relatively few studies of the interactions of synthetic SM with cholesterol or other phospholipids have been performed. With the structure and properties of C18:0-SM well defined (Figs. 1 and 2; see also Maulik et al., 1991), we now describe the interactions of fully hydrated C18:0-SM with cholesterol and DPPC.

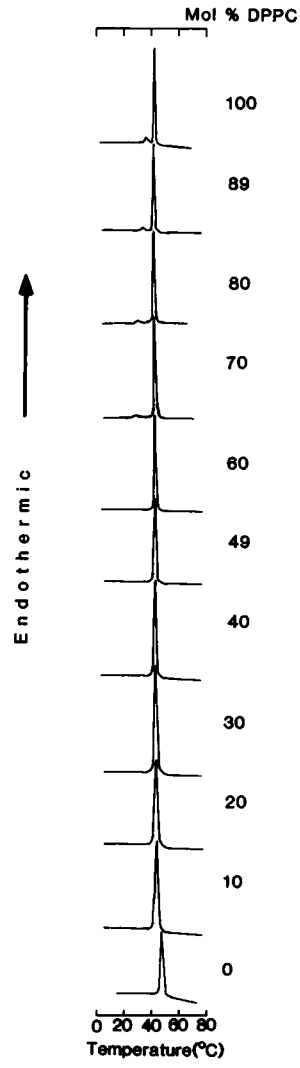

FIGURE 8 DSC heating scans of hydrated (75 wt% water) C18:0-SM containing 0, 10, 20, 30, 40, 50, 60, 70, 80, 89, and 100 mol% DPPC. Heating scan rate, 5°C/min.

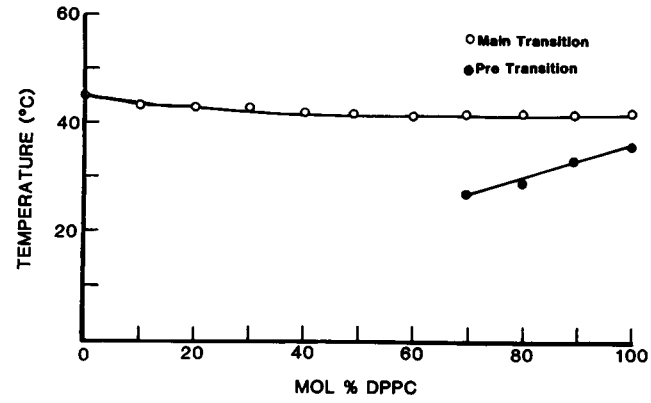

FIGURE 9 Plot of transition temperature of hydrated (75 wt% water) C18:0-SM/DPPC mixtures. ○, Chain-melting transition; ●, pre-transition.

progressively removes the chain-melting transition of C18:0-SM, 2) produces a broad higher temperature transition, and 3) further broadens this higher temperature transition until at >40 mol% cholesterol there is no detectable cooperative transition. The total enthalpy associated with the chain-melting transition of C18:0-SM decreases progressively as the cholesterol content increases and is essentially zero at cholesterol contents of >40 mol%. This calorimetric behavior strongly resembles that observed in our previous calorimetric study of C16:0-SM/cholesterol (Calhoun and Shipley, 1979b). In addition, this behavior is similar to that observed for numerous PC/cholesterol systems (for the original "low sensitivity" DSC study of DPPC/cholesterol, see Ladbrooke et al., 1968). More recent "high sensitivity" DSC studies of DPPC/cholesterol (Estep et al., 1978; Huang et al., 1993; McMullen et al., 1993, 1995; McMullen and McElhaney, 1995) show sharp and broad transitions, and in general, these investigators favor the presence of "cholesterol-rich" and "cholesterol-poor" phases; however, a structural characterization of such phases is lacking. Interestingly, McMullen et al. (1995) observe a change in slope at ~40 mol% cholesterol in the plot of total

C18:0-SM/cholesterol interactions

It has been established that cholesterol serves to regulate phospholipid bilayer fluidity in a state intermediate between the gel and liquid-crystalline phases. In addition, cholesterol appears to have a different affinity for different phospholipids, and SM in particular was reported to have the greatest affinity for sphingomyelin (van Dijck et al., 1976; Demel et al., 1977). Early ^{1}H-NMR and electron spin resonance studies (Oldfield and Chapman, 1971, 1972) showed that addition of cholesterol to the multilamellar liposomes of bovine brain SM fluidizes the bilayer below its transition temperature and makes it less fluid above the transition temperature, as described previously for PC.

In the present study our DSC data (Figs. 3 and 4) show that addition of cholesterol over the range 0–60 mol% 1)

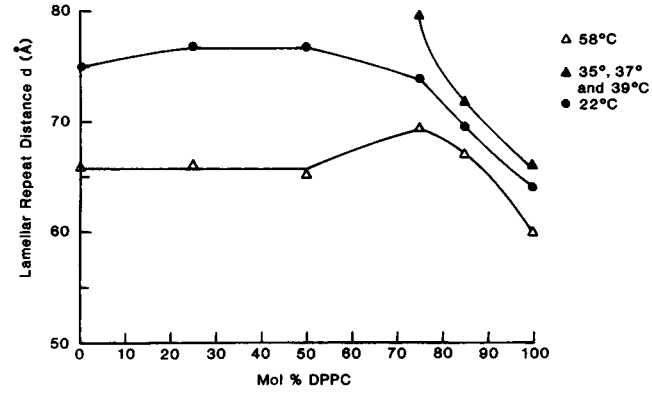

FIGURE 10 Bilayer periodicity, d (Å), of hydrated (50 wt% water) C18:0-SM/DPPC binary mixtures as a function of mol% DPPC. ●, 22°C; ▲, 35–39°C; △, 58°C.

enthalpy versus cholesterol concentration similar to that observed for C18:0-SM/cholesterol (see Fig. 4). However, there is no simple explanation of this behavior. For C18:0-SM/cholesterol at intermediate cholesterol contents (10–20 mol%), the two transitions (the residual chain-melting transition of C18:0-SM at ~43°C and the broad transition at ~46°C) are both observed (see Fig. 3), suggesting some form of lateral phase separation below ~40°C and, perhaps consistent with the idea of "cholesterol-rich" and "cholesterol-poor" phases. However, x-ray diffraction patterns recorded for all C18:0-SM/cholesterol molar ratios at temperatures below the two transitions reveal only a single bilayer phase. Thus, either the two phases (if present) are structurally similar, with the observed diffraction pattern representing some average of the two, or one of the phases is not ordered enough to provide sharp lamellar diffraction. In addition, for all C18:0-SM/cholesterol mixtures the x-ray diffraction data recorded above the transition confirm the presence of only a single bilayer phase.

At 22°C, the sharp wide-angle reflection ($1/4.2Å^{-1}$) indicative of hexagonally packed chains with no chain tilt progressively shifts in position with increasing cholesterol content and becomes diffuse. This provides direct evidence of cholesterol incorporation in the bilayer and perturbation of the hydrocarbon chain packing. Similarly, the broad 1/4.5 $Å^{-1}$ reflection observed at 58°C shifts gradually with increasing cholesterol content, again indicating a gradual alteration of the original liquid-crystalline chain packing.

For C18:0-SM containing 50 mol% cholesterol, the diffraction patterns recorded below and above the original transition temperature are essentially identical in both the low-angle and wide-angle regions. The corresponding electron density profiles show the predicted similarities in both the profile shape (note the peaks at ±10 Å due to cholesterol) and the derived structural parameters (d_{p-p}, d_w) at 22°C and 58°C. The bilayer thickness d_{p-p} for C18:0-SM/50 mol% cholesterol is the same (~46) at both temperatures and intermediate between that observed for hydrated C18:0-SM alone in the gel phase (~52 Å) and the liquid-crystalline phase (~43 Å). Similar changes in bilayer structural parameters and electron density profiles for several PC/cholesterol systems at 20°C were reported by McIntosh (1978), but temperature-dependent changes have not, as far as we are aware, been reported. It is clear that cholesterol induces progressive changes in the bilayer thickness to produce at 50 mol% cholesterol a value intermediate between that observed for the gel and liquid-crystalline phases of C18:0-SM alone.

Thus our present data, obtained from a combination of DSC and x-ray diffraction, define the thermodynamic and structural changes that occur as cholesterol is incorporated into the bilayer matrix of C18:0-SM (see Fig. 11). At 50 mol% cholesterol the cooperative chain-melting transition of C18:0-SM has been removed, and a "temperature-insensitive" bilayer of intermediate structural characteristics (i.e., bilayer thickness and chain packing) is formed. These conclusions are in broad agreement with those of our previous study of C16:0-SM/cholesterol showing complete removal of the chain-melting transition at 42 mol% cholesterol (Calhoun and Shipley, 1979b) and with the high-sensitivity DSC studies of the interactions of cholesterol with C16:0-, C18:0-, and C24:0-SM (Estep et al., 1979, 1981). Estep et al. (1979, 1981) interpreted their calorimetric data in terms of SM/cholesterol systems undergoing phase separation, the sharper DSC transition being due to a phase enriched in SM and the broader component associated in some manner with a phase enriched in cholesterol. As discussed above, although our DSC data also suggest low-temperature phase separation, our x-ray diffraction studies of both the C16:0-SM/cholesterol (Calhoun and Shipley, 1979b) and C18:0-SM/cholesterol systems fail to identify coexisting low-temperature phases.

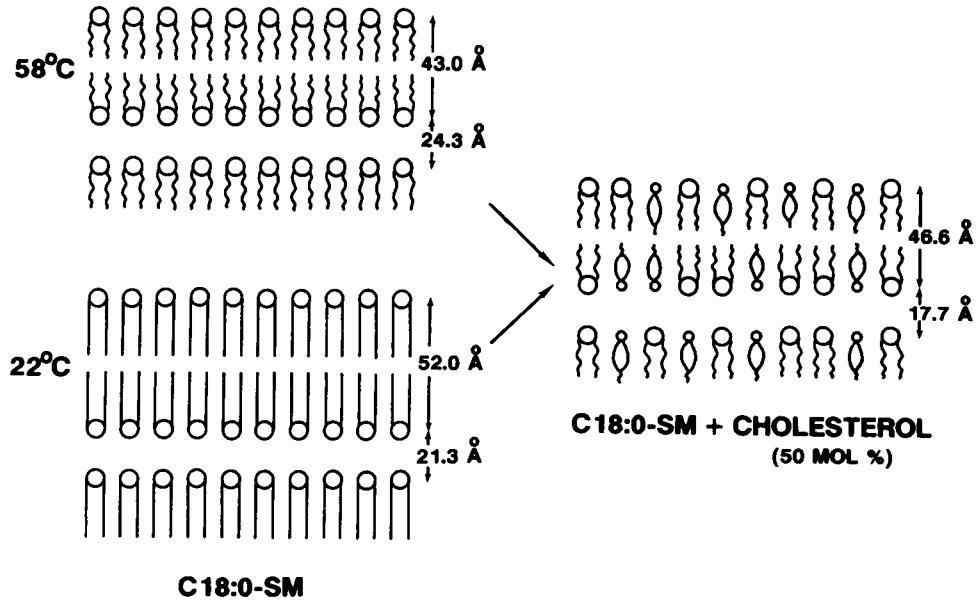

FIGURE 11 Summary of the structural changes exhibited by C18:0-SM (*left*) on incorporation of 50 mol% cholesterol (*right*).

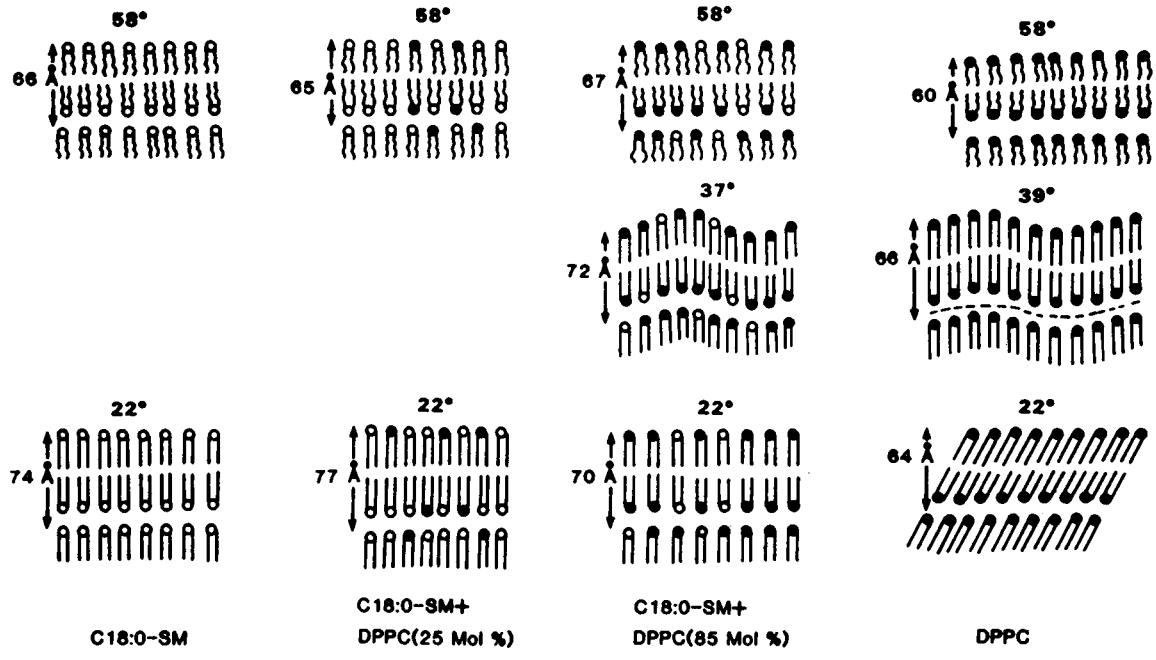

FIGURE 12 Summary of the structural changes exhibited by C18:0-SM (*left*) on incorporation of 25, 85, and 100 mol% DPPC.

Recently McIntosh et al. (1992a,b) have studied the effects of cholesterol on C24:0-SM and bovine brain SM by using DSC and x-ray diffraction methods. Whereas C24:0-SM exhibits a more complex thermotropic behavior with at least two transitions (see also Maulik and Shipley, 1995), again incorporation of 50 mol% cholesterol completely eliminates these transitions; similar behavior was observed for bovine brain SM. At low temperatures, comparison of the electron density profiles of C24:0-SM and bovine brain SM in the absence and presence of 50 mol% cholesterol show effects similar to those shown in Fig. 7, i.e., a change in the shape of the profile and a reduction in $d_{p\text{-}p}$.

C18:0-SM interactions with DPPC

Our previous study of mixtures of natural SM and PC, which differ by ~40°C in their hydrocarbon chain-melting transition temperatures, showed that they form completely miscible phospholipid bilayers at high temperatures and undergo lateral phase separation of the higher melting SM component as the temperature is lowered (Untract and Shipley, 1977). Later studies of mixtures of C16:0-SM and dimyristoyl-PC, where the chain-melting transition temperatures differ by ~17°C, show only a single order-disorder transition at all molar ratios, and miscibility of SM and PC was found in both the gel and liquid-crystalline phases (Calhoun and Shipley, 1979b). Mixtures of C18:0-SM and DPPC, which differ in their chain-melting transitions by 3°C, exhibit a single transition at all molar ratios. As expected, C18:0-SM and DPPC are completely miscible in both the gel and liquid-crystalline phases, and there is no evidence of lateral phase separation. X-ray diffraction data (Fig. 10) demonstrate that lamellar bilayer phases are present at all C18:0-SM/DPPC molar ratios. A decrease in bilayer periodicity is observed for both the low (gel) and high (liquid-crystalline) temperature phases at DPPC contents of >70 mol%, possibly because of increased chain tilt for DPPC-rich gel phase bilayers or differences in the hydration limits of C18:0-SM and DPPC. The structural changes exhibited by C18:0-SM with increasing DPPC content are summarized in Fig. 12.

The studies described here pave the way for future efforts to address the issue of cholesterol interactions in mixed SM/PC bilayer systems. In particular, the question of whether cholesterol interacts with higher affinity with SM than with PC (or other phospholipids) must be answered. This could be relevant to the potential use of SM-containing bilayer vesicles as efficient vehicles for the removal of cholesterol from cells (Lund-Katz et al., 1988).

We thank Dr. Pavanaram Sripada for the synthesis of C18:0-SM, David Jackson for technical assistance, and Dr. David Atkinson for helpful advice. We also thank Irene Miller for help in preparing the manuscript.

This research was supported by research grant HL-26335 and training grant HL-07291 from the National Institutes of Health.

REFERENCES

Ahmad, T. Y., J. T. Sparrow, and J. D. Morrisett. 1985. Fluorine-, pyrene- and nitroxide-labeled sphingomyelin: semi-synthesis and thermotropic properties. *J. Lipid Res.* 25:1160–1165.

Barenholz, Y., and S. Gatt. 1982. Sphingomyelin: metabolism, chemical synthesis, chemical and physical properties. *In* Phospholipids. J. N. Hawthorne and G. B. Ansell, editors. Elsevier, Amsterdam. 129–177.

Barenholz, Y., J. Suurkuusk, D. B. Mountcastle, T. E. Thompson, and R. L. Biltonen. 1976. A calorimetric study of the thermotropic behavior of aqueous dispersions of natural and synthetic sphingomyelins. *Biochemistry.* 15:2441–2447.

Barenholz, Y., and T. E. Thompson. 1980. Sphingomyelins in bilayers and biological membranes. *Biochim. Biophys. Acta.* 604:129–158.

Bruzik, K. S. 1988a. Synthesis and spectral properties of chemically and stereochemically homogeneous sphingomyelin and its analogues. *J. Chem. Soc. (Perkin 1).* 423–431.

Bruzik, K. S. 1988b. Conformation of the polar headgroup of sphingomyelin and its analogues. *Biochim. Biophys. Acta.* 939:315–326.

Bruzik, K. S., B. Sobon, and G. M. Salamonczyk. 1990. Nuclear magnetic resonance study of sphingomyelin bilayers. *Biochemistry.* 29: 4017–4021.

Bruzik, K. S., and M-D. Tsai. 1987. A calorimetric study of the thermotropic behavior of pure sphingomyelin diastereomers. *Biochemistry.* 26:5364–5368.

Calhoun, W. I., and G. G. Shipley. 1979a. Fatty acid composition and thermal behavior of natural sphingomyelins. *Biochim. Biophys. Acta.* 555:435–441.

Calhoun, W. I., and G. G. Shipley. 1979b. Sphingomyelin-lecithin bilayers and their interaction with cholesterol. *Biochemistry.* 18:1717–1722.

Cohen, R., Y. Barenholz, S. Gatt, and A. Dagan. 1984. Preparation and characterization of well defined D-erythro sphingomyelins. *Chem. Phys. Lipids.* 35:371–384.

Demel, R. A., J. W. C. H. Jansen, P. W. M. van Dijck, and L. L. M. van Deenen. 1977. The preferential interaction of cholesterol with different classes of phospholipids. *Biochim. Biophys. Acta.* 465:1–10.

Dong, Z., and J. A. Butcher. 1993. An efficient route to *N*-palmitoyl-D-erythro-sphingomyelin and its ^{13}C-labeled derivatives. *Chem. Phys. Lipids.* 66:41–46.

Elliott, A. J. 1965. The use of toroidal reflecting surfaces in x-ray diffraction cameras. *J. Sci. Instrum.* 42:312–316.

Estep, T. N., W. I. Calhoun, Y. Barenholz, R. L. Biltonen, G. G. Shipley, and T. E. Thompson. 1980. Evidence for metastability in stearoylsphingomyelin bilayers. *Biochemistry.* 19:20–24.

Estep, T. N., E. Freire, D. B. Mountcastle, Y. Barenholz, R. L. Biltonen, and T. E. Thompson. 1981. Thermal behavior of stearoylsphingomyelin-cholesterol dispersions. *Biochemistry.* 20:7115–7119.

Estep, T. N., D. B. Mountcastle, Y. Barenholz, R. L. Biltonen, and T. E. Thompson. 1979. Thermal behavior of synthetic sphingomyelin-cholesterol dispersions. *Biochemistry.* 18:2112–2117.

Estep, T. N., D. B. Mountcastle, R. L. Biltonen, and T. E. Thompson. 1978. Studies on the anomalous thermotropic behavior of aqueous dispersions of dipalmitoylphosphatidylcholine-cholesterol mixtures. *Biochemistry.* 17:1984–1989.

Franks, A. 1958. Some developments and applications of microfocus x-ray diffraction techniques. *Br. J. Appl. Phys.* 9:349–352.

Hannun, Y. A. 1994. The sphingomyelin cycle and the second messenger function of ceramide. *J. Biol. Chem.* 269:3125–3128.

Hannun, Y. A., and L. M. Obeid. 1995. Ceramide: an intracellular signal for apoptosis. *Trends Biochem. Sci.* 20:73–77.

Huang, T.-H., C. W. B. Lee, S. K. Das Gupta, A. Blume, and R. G. Griffin. 1993. A ^{13}C and ^{2}H nuclear magnetic resonance study of phosphatidylcholine/cholesterol interactions: characterization of liquid-gel phases. *Biochemistry.* 32:13277–13287.

Khare, R. S., and C. R. Worthington. 1977. An x-ray diffraction study of sphingomyelin-cholesterol interaction in oriented bilayers. *Mol. Cryst. Liq. Cryst.* 38:195–206.

Ladbrooke, B. D., R. M. Williams, and D. Chapman. 1968. Studies on lecithin-cholesterol-water interactions by differential scanning calorimetry and x-ray diffraction. *Biochim. Biophys. Acta.* 150:333–340.

Long, R. A., F. E. Hruska, H. D. Gesser, and J. C. Hsia. 1971. Phase transitions in sphingomyelin thin films. A spin label study. *Biochem. Biophys. Res. Commun.* 45:167–173.

Lund-Katz, S., H. M. Laboda, L. R. McLean, and M. C. Phillips. 1988. Influence of molecular packing and phospholipid type on rates of cholesterol exchange. *Biochemistry.* 27:3416–3423.

Maulik, P. R., D. Atkinson, and G. G. Shipley. 1986. X-ray scattering of vesicles of *N*-acyl sphingomyelins: determination of bilayer thickness. *Biophys. J.* 50:1071–1077.

Maulik, P. R., and G. G. Shipley. 1995. X-ray diffraction and calorimetric study of *N*-lignoceryl sphingomyelin membranes. *Biophys. J.* 69: 1909–1916.

Maulik, P. R., P. K. Sripada, and G. G. Shipley. 1991. Structure and thermotropic properties of hydrated *N*-stearoyl sphingomyelin bilayer membranes. *Biochim. Biophys. Acta.* 1062:211–219.

McIntosh, T. J. 1978. The effect of cholesterol on the structure of phosphatidylcholine bilayers. *Biochim. Biophys. Acta.* 513:43–58.

McIntosh, T. J., S. A. Simon, D. Needham, and C. Huang. 1992a. Structure and cohesive properties of sphingomyelin/cholesterol bilayers. *Biochemistry.* 31:2012–2020.

McIntosh, T. J., S. A. Simon, D. Needham, and C. Huang. 1992b. Interbilayer interactions between sphingomyelin and sphingomyelin/cholesterol bilayers. *Biochemistry.* 31:2020–2024.

McMullen, T. P. W., and R. N. McElhaney. 1995. New aspects of the interaction of cholesterol with dipalmitoylphosphatidylcholine bilayers as revealed by high-sensitivity differential scanning calorimetry. *Biochim. Biophys. Acta.* 1234:90–98.

McMullen, T. P. W., R. N. A. H. Lewis, and R. N. McElhaney. 1993. Differential scanning calorimetric study of the effect of cholesterol on the thermotropic phase behavior of a homologous series of linear saturated phosphatidylcholines. *Biochemistry.* 32:516–522.

McMullen, T. P. W., C. Vilcheze, R. N. McElhaney, and R. Bittman. 1995. Differential scanning calorimetric study of the effect of sterol side chain length and structure on dipalmitoylphosphatidylcholine thermotropic phase behavior. *Biophys. J.* 69:169–176.

Nieva, J. L., R. Bron, J. Corver, and J. Wilschut. 1994. Membrane fusion of Semliki forest virus requires sphingolipids in the target membrane. *EMBO J.* 13:2797–2804.

Oldfield, E., and D. Chapman. 1971. Effects of cholesterol and cholesterol derivatives on hydrocarbon chain mobility in lipids. *Biochem. Biophys. Res. Commun.* 43:610–616.

Oldfield, E., and D. Chapman. 1972. Molecular dynamics of cerebroside-cholesterol and sphingomyelin-cholesterol interactions: implications for myelin membrane structure. *FEBS Lett.* 21:303–306.

Shapiro, D. 1969. Chemistry of Sphingolipids. Hermann, Paris.

Shipley, G. G., L. S. Avecilla, and D. M. Small. 1974. Phase behavior and structure of aqueous dispersions of sphingomyelin. *J. Lipid Res.* 15: 124–131.

Sripada, P. K., P. R. Maulik, J. A. Hamilton, and G. G. Shipley. 1987. Partial synthesis and properties of a series of *N*-acyl sphingomyelins. *J. Lipid Res.* 28:710–718.

Untracht, S. M., and G. G. Shipley. 1977. Molecular interactions between lecithin and sphingomyelin: temperature- and composition-dependent phase separation. *J. Biol. Chem.* 252:4449–4457.

van Dijck, P. W. M., B. de Kruijff, L. L. M. van Deenen, J. de Gier, and R. A. Demel. 1976. The preference of cholesterol for phosphatidylcholine in mixed phosphatidylcholine-phosphatidylethanolamine bilayers. *Biochim. Biophys. Acta.* 455:576–587.

Worthington, C. R., and A. E. Blaurock. 1969. A structural analysis of nerve myelin. *Biophys. J.* 9:970–990.